Korean Chem. Eng. Res., 54(1), 127-134 (2016)
http://dx.doi.org/10.9713/kcer.2016.54.1.127
PISSN 0304-128X, EISSN 2233-9558

Synthesis, Characterization and Photocatalytic Activity of Reduced Graphene Oxide-Ce/ZnO Composites

Wenjun Zhang†, Jinfeng Zhao and Xuefeng Zou

School of Chemical Engineering and Technology, Hebei University of Technology, Tianjin 300130, PR China
(Received 13 January 2015; Received in revised form 24 April 2015; accepted 28 May 2015)

Abstract – A series of Ce-doped ZnO (Ce/ZnO) nanostructures were fabricated using the co-precipitation method, then a simply nontoxic hydrothermal approach was proposed for preparation of reduced graphene oxide (rGO)-Ce/ZnO composites. The synthesized composites were investigated by powder X-ray diffraction (XRD), scanning electron microscopy (SEM), Fourier transform infrared spectroscopy (FT-IR), photoluminescence spectroscopy (PL), electrochemical impedance spectroscopy (EIS), UV-vis diffuse reflectance spectroscopy (DRS) techniques and Raman pattern. The as-synthesized rGO-Ce/ZnO composites showed high photodecomposition efficiency in comparison with the rGO-ZnO, Ce/ZnO, pure ZnO under UV, visible-light and sunlight irradiation. The degradation of methylene blue (MB) (10 mg/L, 100ml) by 95.8% within 60 min by using rGO-2 (10 mg) under sunlight irradiation was observed. The repeated use of the rGO-2 was investigated, and the results showed almost no decay in the catalytic activity.

Key words: rGO, Ce/ZnO, Photocatalysis, MB

1. Introduction

Organic dyes and pigments from printing, textiles, and dyeing industries are resistant to biological degradation and can affect the environment by the release of toxic, carcinogenic, and colored wastewater [1]. Photocatalysis as a promising method to solve environmental pollution problems has been a hot research topic due to its mild reaction condition, high degradation, broad applied area and facile manipulation [2-4]. The mechanism of photocatalysis is as follows: First, metal oxide semiconductor photocatalyst absorbs the light of specific wavelengths to produce electron-hole pairs; Secondly, the great mass of these electron-hole pairs recombine rapidly while only a small part of them transferring to the surface of photocatalyst can be used for degradation reactions [5-8]. It is well documented that semiconductor ZnO is a suitable alternative to the traditional photoactive semiconductor TiO_2 due to its low cost, nontoxicity and high chemical stability [9,10]. However, owing to its a small fraction of 4% of the solar spectrum, larger band gap (3.2eV), high recombination rate of photo-generated electron-hole pairs and photocorrosion effects during light irradiation [11,12], the photocatalytic efficiency of ZnO remains relatively low. Hence, restraining electron-hole pair recombination of ZnO plays an important role to improve its photocatalysis performance. Many works have been done to enhance the photocatalytic activity of ZnO [13,14]. Li *et al*. [14] synthesized ZnO with various morphologies, including column-like, grenade-like, rod-like, spindle-like, flower-like and shuttle-like micro-/nanostructures, and the results showed that the spindle-like photocatalyst exhibited the maximum photocatalytic activity. It has been also reported that doping of Eu^{3+}, Ce, Fe^{3+}, and Ag can improve the photocatalytic performance of semiconductor ZnO, for these can act as electron trapping agents to restrain electron hole recombination rate [15-19]. Among doped nanostructures, great efforts have been made to explore for potential applications in various fields due to the miscellaneous properties of Ce/ZnO nanostructures [20-26]. Ce/ZnO nanocomposition has been synthesized and studied for degradation of a variety of dyes, infrared emissivity, detoxification of cyanide and so on.

Graphene has attracted researchers' interest owing to its honeycomb network structure after its pioneering isolation in 2004. Graphene oxide (GO) possesses abundant hydroxyl, carboxyl, epoxy, carbonyl groups, which can offer a platform for semiconductor metal-oxide. When rGO acts as a support material of photocatalyst, it can effectively suppress the recombination of photo-generated charge carriers. Meanwhile, it shows extraordinary adsorption for dye molecules via a higher specific surface area. These outstanding characteristics make rGO become the rising star in photocatalysis [27,28]. Li *et al*. [29] prepared rGO/potassium niobate composite nanoscrolls as a photocatalyst, which showed high photocatalytic activity for dye degradation. Furthermore, using rGO as support material to enhance the photocatalytic activity of ZnO has been discussed intensively [30-35]. Some reports have also discussed synergetic effects of the metal and rGO in the process of photocatalytic [7,36]. Several works have investigated the preparation and properties of graphene-based composite materials, and it was found that composite photocatalyst shows enhanced photocatalytic activity. To the best of our knowledge, the photodegradation of MB using Ce doped ZnO and reduced

† To whom correspondence should be addressed.
E-mail: wjzhang@hebut.edu.cn

graphene oxide materials has been seldom addressed.

In this paper, a series of Ce/ZnO nanostructures were synthetized using the co-precipitation method and then a simple nontoxic hydrothermal approach was proposed for preparation of visible-light-responsive rGO-Ce/ZnO composites. The as-synthesized rGO-Ce/ZnO composites showed high photocatalytic degradation efficiency of methylene blue (MB) compared to the Ce/ZnO, pure ZnO under UV, visible-light and sunlight irradiation. The synergetic effects of the metal and rGO have also been discussed.

2. Experimental

2-1. Materials and reagents

Natural graphite powder was obtained from Qingdao Jinrilai graphite Corporation. Hydrogen peroxide (H_2O_2, 30%) was obtained from Tianjin Bot Chemical Corporation. Sodium nitrate ($NaNO_3$) was supplied by Tianjin Viktor Chemical Corporation. Zinc nitrate 6-hydrate ($Zn(NO_3)_2 \cdot 6H_2O$) was purchased from Tianjin Guangfu Science and Technology Development Corporation. Cerium nitrate 6-hydrate ($Ce(NO_3)_3 \cdot 6H_2O$) was supplied by Tianjin Jingke Institute of Fine Chemicals. Methylene blue (MB) was obtained from Tianjin Bodi Chemical Corporation. Potassium permanganate ($KMnO_4$) was supplied by Tianjin Jiangtian Chemical Corporation. All reagents were analytical grade without further treatment. Distilled water was used in the experiment.

2-2. Preparation of graphite oxide

Graphite oxide (GO) was synthesized according to an improved Hummers' method [37]. Graphite powder (1.0 g) and $NaNO_3$ (0.5 g) were slowly added into H_2SO_4 (98% wt, 23ml) while stirring in an ice bath for 0.5 h. Then, $KMnO_4$ (3.0 g) was slowly added to the mixture for about 15 minutes. The mixture was under continuous stirring for 2 h in an ice bath. Subsequently, the temperature was increased to 35 ^oC and kept for 0.5 h, followed by the addition of distilled water (46 ml). The flask was kept at 98 ^oC for 15 min with more distilled water added into the mixture. H_2O_2 (10 ml) was added into the resulting dark-brown paste. The resultant product was centrifuged and the precipitation was washed with a dilute acid solution (5% wt, HCl) for five times and distilled water until the pH value reached the neutral level of 5~6. Finally, the production was dried in oven at 50 ^oC for 8h.

2-3. Preparation of Ce/ZnO

Typically, Zn $(NO_3)_2 \cdot 6H_2O$ (7.437 g) and a given amount of Ce $(NO_3)_3 \cdot 6H_2O$ were dissolved in 50 ml of distilled water under stirring. NaOH (2.000 g) dissolved in deionized water (50 ml) was added to the mixture slowly and stirred for 30 minutes to obtain a homogeneous mixture. The nanostructures were recovered using vacuum suction filtration, washed with ethanol and deionized water for three times. The products were dried at 50 ^oC for 12 h. Those powders were obtained after the calcination of precipitates at 600 ^oC for 2 h. Three samples were synthesized with mass ratio of Ce: ZnO of 0:100, 2:100, 4:100, noted as ZnO, 2Ce/ZnO, 4Ce/ZnO.

2-4. Synthesis of rGO-Ce/ZnO photocatalysts

The rGO-ZnO was synthesized via a hydrothermal method according to the procedure described in reference [38]. In a typical procedure, 40 mg of GO was exfoliated in a solution of distilled water (60 mL) to form a homogeneous suspension by ultrasonic dispersion for 30 min. 0.4 g ZnO was added. The mixture was stirred for 2 h to get a uniform suspension. The mixing solution was transferred into a 100 ml Teflon-lined container and maintained at 120 ^oC for 3 h. rGO-ZnO composite was recovered by centrifugation and washed with distilled water for three times after the autoclave cooled to room temperature. Finally, the production was dried in air at 50 ^oC for 8 h. For comparison, another two samples were synthesized by the same condition, only with 2Ce/ZnO and 4Ce/ZnO instead of ZnO, noted as rGO-2, rGO-4, respectively.

2-5. Characterization

X-ray diffraction (XRD) patterns were obtained using Germany Bruker AX in the range of 5~90^o. The surface morphology and particle size were observed with a scanning electron microscope (SEM, FEI, NVOA NANASEM 450). Fourier transform infrared (FT-IR) analysis was recorded on a Germany Bruker Tensor27 spectrometer between 4000 and 400 cm^{-1}. The DRS spectra were done on a UV-vis spectrophotometer (Agilent, Cary100). Photoluminescence (PL) emission spectra were determined using a HITACHI F-4600 Fluorescence spectrophotometer with 325 nm wavelength incident laser light at room temperature.

2-6. Photocatalytic degradation of MB

The adsorptivity and photocatalytic properties of the synthetic compounds were evaluated for the decomposition of MB under the irradiation of UV (λ=365 nm), visible light (λ>420 nm, 500W Xe lamp) and natural sunlight. To ensure similar conditions, all photocatalytic experiments were on sunny days between 11:00 a.m. to 12:00 a.m. in June. In a typical process, the photocatalysts (10 mg) were added into MB aqueous solution (10 mg/L, 100 mL). To reach an adsorption-desorption equilibrium of dyes on the photocatalyst surface, the suspensions were kept stirred in the dark for 0.5 h. Then the suspensions were exposed to light irradiation. Then 5 mL of solution was taken out at a given time interval and centrifuged to measure the concentration of MB with a UV-Vis spectrophotometer.

3. Result and Discussion

3-1. Characterizations of prepared materials

Fig. 1 shows the XRD patterns of GO, pure ZnO, 2Ce/ZnO, 4Ce/ZnO, rGO-ZnO, rGO-2, and rGO-4. For as-prepared GO, an intense and sharp peak at 9.8^o was observed which can be attributed to the (002) diffraction. Secondly, the diffraction peaks in pure ZnO are well indexed with (JCPDS NO.36-1451) of bulk ZnO of hexagonal

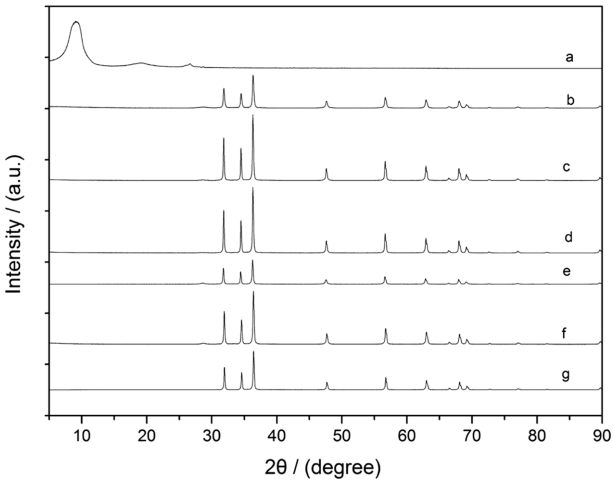

Fig. 1. (a) XRD spectra of (a) GO, (b) rGO-4, (c) rGO-2, (d) rGO-ZnO, (e) 4Ce-ZnO, (f) 2Ce-ZnO, (g) ZnO.

wurtzite phase. These peaks correspond to the reflections from (100), (002), (101), (102) and (103) at 2θ values of approximately 31.8°, 34.4°, 36.3°, 47.6° and 62.9°, respectively. The XRD patterns of the rGO-Ce/ZnO composites and rGO-ZnO present no obvious peaks take shift after GO added, demonstrating GO has a weak effect on the crystal phase of ZnO, which can be explained by the destroyed regular stack of GO due to the intercalation of ZnO or Ce/ZnO. Nevertheless, the Ce doped samples exhibited additional diffraction peaks located at 2θ=28.7° which could be indexed to the (111) plane for the cubic CeO_2 crystalline. According to the Scherrer formula, these results show that the Ce/ZnO nanoparticles are decorated on the rGO sheets with a size of 45~50 nm.

Fig. 2 represents the SEM images of the morphology of composites. The 2D rGO sheets are clearly observed from Fig. 2(a). The 2D rGO sheets exhibit intrinsic microscopic roughening and wrinkles with not perfectly flat. Uniform spherical-like particles are clearly observed from Fig. 2(b), (c). The SEM images of rGO-2 in Fig. 2(d), (e) exhibit close encounters between rGO and 2Ce/ZnO. Those nanoparticles are randomly distributed and firmly anchored on the wrinkled rGO sheets. In particular, abundant oxygen-containing groups in GO can serve as anchoring sites for 2Ce/ZnO [38]. On one hand, this would be beneficial to improve the dispersibility of 2Ce/ZnO on rGO; on the other hand, the nanoparticles may hinder rGO sheets against aggregation. The SEM images of the ZnO and Ce/ZnO reveal that the products consist of highly uniform nanoparticles with the diameter of 45~50 nm, respectively, which is in agreement with results from XRD.

Fig. 3 shows the FT-IR spectra of (a) GO, (b) ZnO, (c) 2Ce/ZnO, (d) 4Ce/ZnO, (e) rGO-0, (f) rGO-2, (e) rGO-4. For GO, the stretching of O-H, the stretching of C=O, the C=C stretching of stretching of the benzenoid rings and Ph, the stretching of C-O-C are observed from the characteristic bands at 3420, 1741, 1625, 1051 cm^{-1}, respectively. A sharp band at 478 cm^{-1} is attributed to the vibrations of ZnO in the FT-IR spectra of the prepared composites, indicating the presence of ZnO. The rGO-Ce/ZnO composites have similar FT-IR profiles, con-

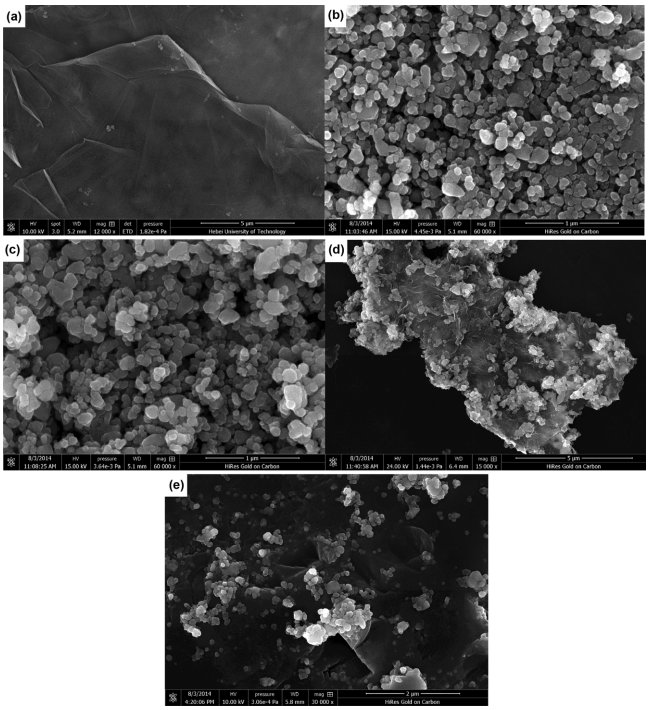

Fig. 2. SEM images of (a) GO, (b) ZnO, (c) 2Ce/ZnO, (d) rGO-2; lower magnification (e) rGO-2; higher magnification.

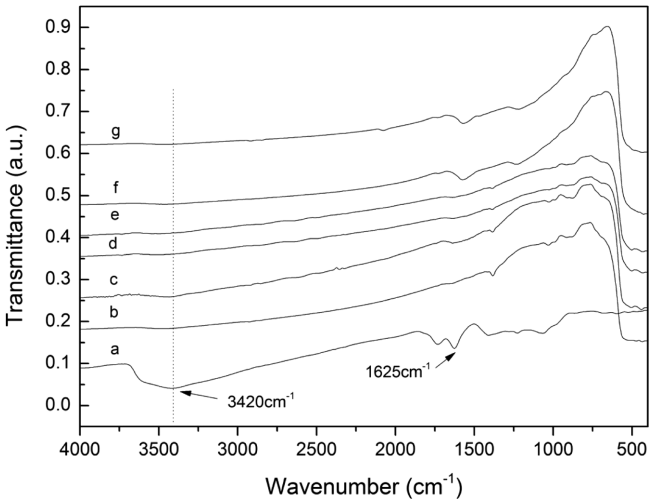

Fig. 3. FT-IR spectra of (a) GO, (b) ZnO, (c) 2Ce/ZnO, (d) 4Ce/ZnO, (e) rGO-ZnO, (f) rGO-2, (f) rGO-4.

firming the existence of rGO and ZnO. However, the band at 1741 cm^{-1} for C=O is almost entirely eliminated and the peaks at 3456 cm^{-1} (O-H), 1725 cm^{-1} (C=O), and 1413 cm^{-1} (C-O) present an obvious decrease, indicating that the oxygen-containing functional groups of GO have been reduced during the hydrothermal process [39].

Photoluminescence (PL) is closely related to the separation and recombination of electrons and holes. PL emission is caused by the radiative recombination of electron and hole. Fig. 4 shows the PL emission intensity of (a) ZnO, (b) 2Ce/ZnO, (c) rGO-ZnO, (d) rGO-2 at room temperature. A UV emission at 410 nm and a broader emission at 470 nm are recorded in Fig. 4(a). The former is due to the

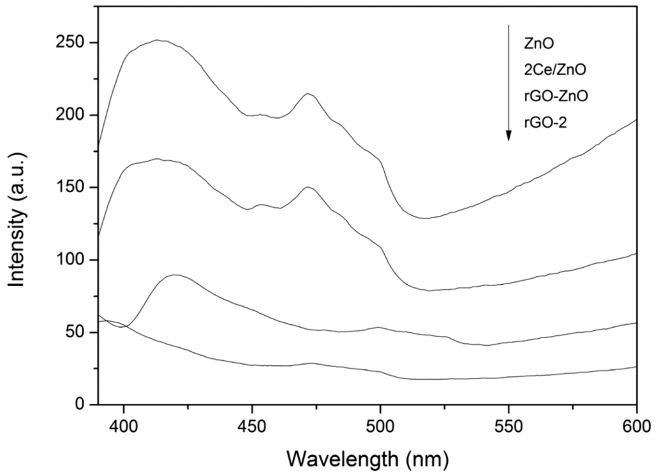

Fig. 4. PL spectra of (a) ZnO, (b) 2Ce/ZnO, (c) rGO-ZnO, (d) rGO-2.

recombination of photogenerated electron-hole pairs near the band edges, and the latter is attributed to arising from surface defects [40,41]. The pure ZnO presents a stronger luminescence emission, indicating a high recombination rate of electron and hole. For Ce/ZnO, the PL spectra decreased, implying that doping Ce suppressed the recombination of photogenerated charge carriers effectively. In particular, the lowest intensity was observed for rGO-2 composite, suggesting that the recombination of photogenerated charge carriers was suppressed due to the cooperative effect of Ce and rGO.

The optical properties of prepared materials were probed by UV-Vis diffuse reflectance spectroscopy, measured in the range of 200~800 nm (Fig. 5a). For ZnO and Ce/ZnO, the absorption bands show an absorption sharp edge rising at 400 nm, which is the characteristic spectrum of ZnO. Compared with them, the spectrum of rGO-2 or rGO-4 displays a slight red-shift to higher wavelength and more intensive absorption in the visible-light region. First, the enhanced absorptivity and slight red shift were due to the presence of crystalline CeO_2 on the nanoparticles and the incorporation of Ce^{4+} ions into the ZnO lattice sites. Second, the addition of rGO into the composite samples modified the optical properties of Ce/ZnO, similar to P25-Graphene composites [42]. The band gap energy of ZnO and rGO-2 is determined to be 3.14 eV and 3.07 eV, respectively. In addition, from Fig. 5(c), we observed that the value of Eg is decreased, suggesting that the rGO-2 can absorb the visible light irradiation slightly better than rGO-ZnO. This means the composites might be prone to be excited by visible light, which is significant for photocatalyst used under sunlight [43].

To understand and determine the number and orientation of layer, quality, and types of edge of the samples, Raman analysis was used to study the rGO and GO materials. Due to elastically scattering charge

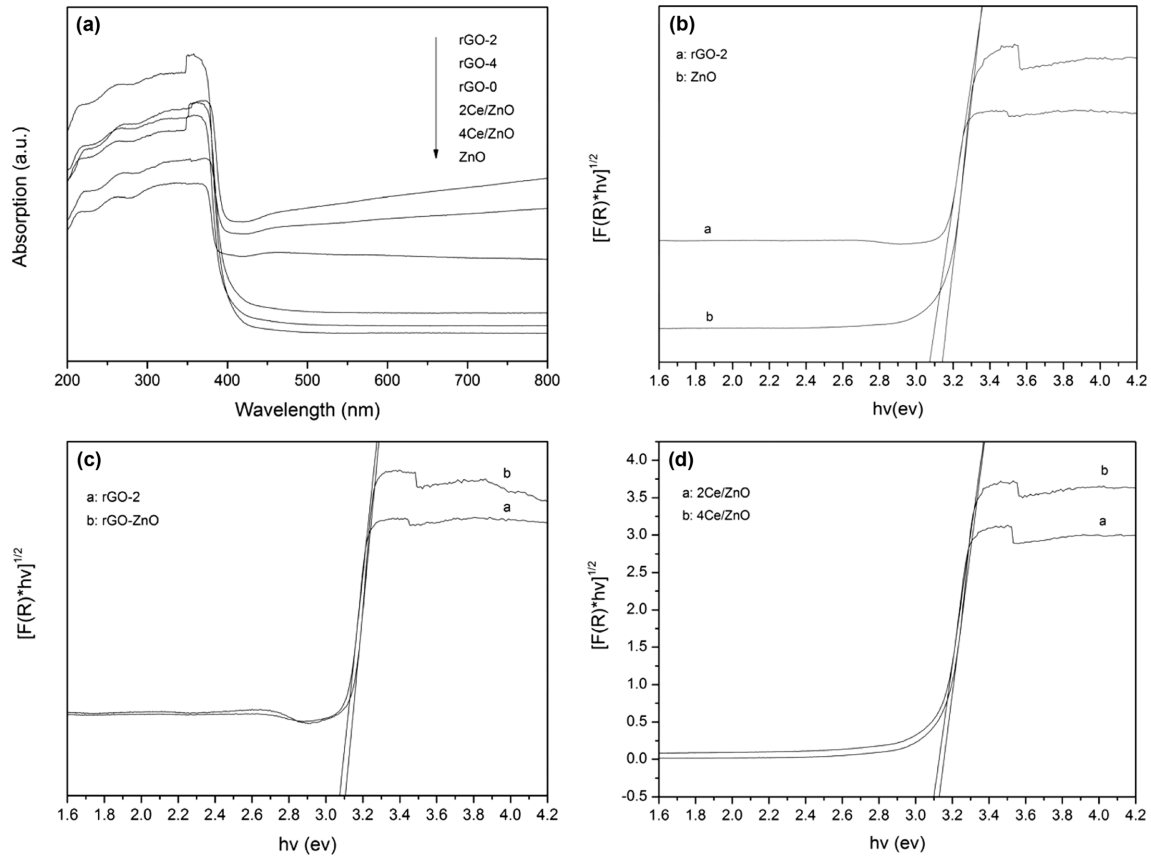

Fig. 5. (a) UV-vis diffuse reflectance spectra of prepared materials (b) Plots of $[F(R)*hv]^{1/2}$ versus energy (hv) for the band gap energy of ZnO and rGO-2. (c) Plots of $[F(R)*hv]^{1/2}$ versus energy (hv) for the band gap energy of (a) rGO-ZnO and (b) rGO-2 (d) Plots of $[F(R)*hv]^{1/2}$ versus energy (hv) for the band gap energy of (a) 2Ce/ZnO and (b) 4Ce/ZnO.

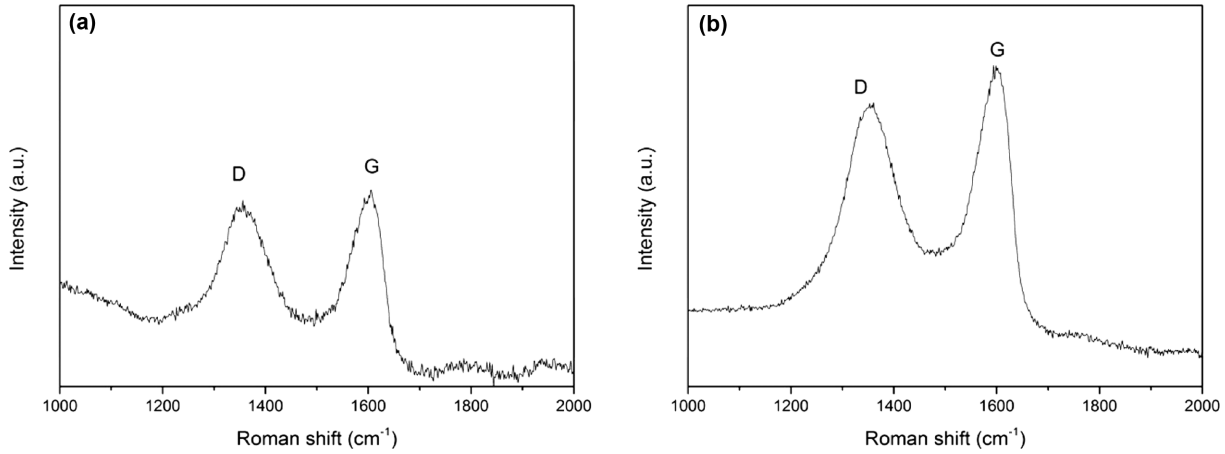

Fig. 6. Raman spectra of (a) GO and (b) rGO samples.

carriers, the major band position in the Raman spectra was significantly changed after hydrothermal process for GO. As shown in Fig. 6, two major vibration bands in the range between 1100 and 1700 cm^{-1} were detected. Clearly, rGO shows a D band at 1350 and a G band at 1593 cm^{-1} while the corresponding bands of GO at 1352 and 1604 cm^{-1}, respectively. Owing to the high ability for recovery of the hexagonal network of carbon atom, the G band of rGO red-shifts from 1603 to 1594 cm^{-1}. Moreover, the intensity ratio of the D band to the G band (I_D/I_G) increased the intensity vibration band after the reduction of GO. The high intensity of G vibration band also indicated that reduced graphene oxide obtained more isolated domains in rGO than in GO. Because of the removal of oxygen moieties from GO, the G vibration band of rGO increased. The D vibration band of rGO increased mainly because of the sp^2 carbon orientation [44].

3-2. Photocatalytic degradation of prepared materials

To determine and compare the photocatalytic performance of ZnO, Ce/ZnO nanoparticles and rGO-Ce/ZnO composites, a series of experiments were carried out using MB under UV, visible, sunlight light irradiation. As shown in Fig. 6(a~c), all of the doped ZnO samples proceed much more rapidly than ZnO. Before the addition of GO, the photocatalytic property of 2Ce/ZnO was confirmed to be the most active, which shows about 87.9%, 90.7%,12.9% higher than the pure ZnO sample under the irradiation of UV, visible sunlight, respectively. Through the data statistics and analysis of Fig. 6(a~c), we concluded that the higher content of Ce could be adverse to enhance the photocatalytic performances, so the mass ratio of Ce/ZnO were 2:100 is the optimum concentration. The photocatalytic activity of rGO-0, rGO-2 or rGO-4 improved dramatically with the addition of GO. In the dark, the composites adsorb MB dyes due to the two-dimensional planar structure. In the photocatalytic process, rGO transport photoelectron simultaneously giant π-π conjugation system, which is resulting from the reduction of GO into rGO. Furthermore, the photocatalytic activity of the rGO-2 under sunlight irradiation was the most excellent; this could offer a considerable potential for sorely needed wastewater treatment. The order of degradation rate of MB is as follows: rGO-2 > rGO-4 > rGO-ZnO > 2Ce/ZnO > 4Ce/ZnO > ZnO under irradiation of UV, visible, sunlight.

To test the photostability of composite, we used rGO-2 as catalyst under sunlight for five times. Fig. 7 shows that after five continuous cycles of degradation MB tests, the photocatalytic activity of the composite did not decrease remarkably, indicating that the composite was extremely stable in photocatalytic process.

3-3. Mechanism

During the photocatalytic process, the sufficient contact between organic dyes and photocatalysts is an important factor for realizing higher photocatalytic performance for the photocatalytic decomposition of organic dyes which usually takes place on the surface of a photocatalyst. The enhanced photocatalytic of the prepared composites toward the MB degradation can be also attributed to the enhanced adsorption capacity of MB dyes of the rGO due to the two-dimensional planar structure, giant π-π conjugation system and huge specific surface area. The rGO of the composites can also serve as an electron reservoir which can prompt the separation of photo-generated electron-hole pairs efficiently. Besides, the narrowed band gap energy of rGO-2 extends the light responsive range of the composites [43]. The photocatalytic activity of ZnO was enhanced by the addition of Ce. Cerium traps electrons, which restrained electron-hole recombination and increasing $O_2^{\cdot-}$ for degradation of organic dyes [45]. However the higher content of Ce could be detrimental to the photocatalytic performance for it may act as recombination center of electrons and holes and photocatalytic activity decreases. Hence, the mass ratio of Ce/ZnO 2:100 is the optimum amount. Furthermore, it has been reported that dyes can act as a sensitizer of visible light. When under light irradiation, the dyes excited electrons, which can be transferred to the conduction band of ZnO and then it becomes a cationic dye radical [41]. Those cationic dye radicals could degrade by the reactive oxidation species or self-degradation. When it comes to the rGO-Ce/ZnO composites, valence electrons of ZnO can be excited to the conduction band leaving behind a hole in the valance band by absorbing visible light due to the Ce/ZnO. These electrons

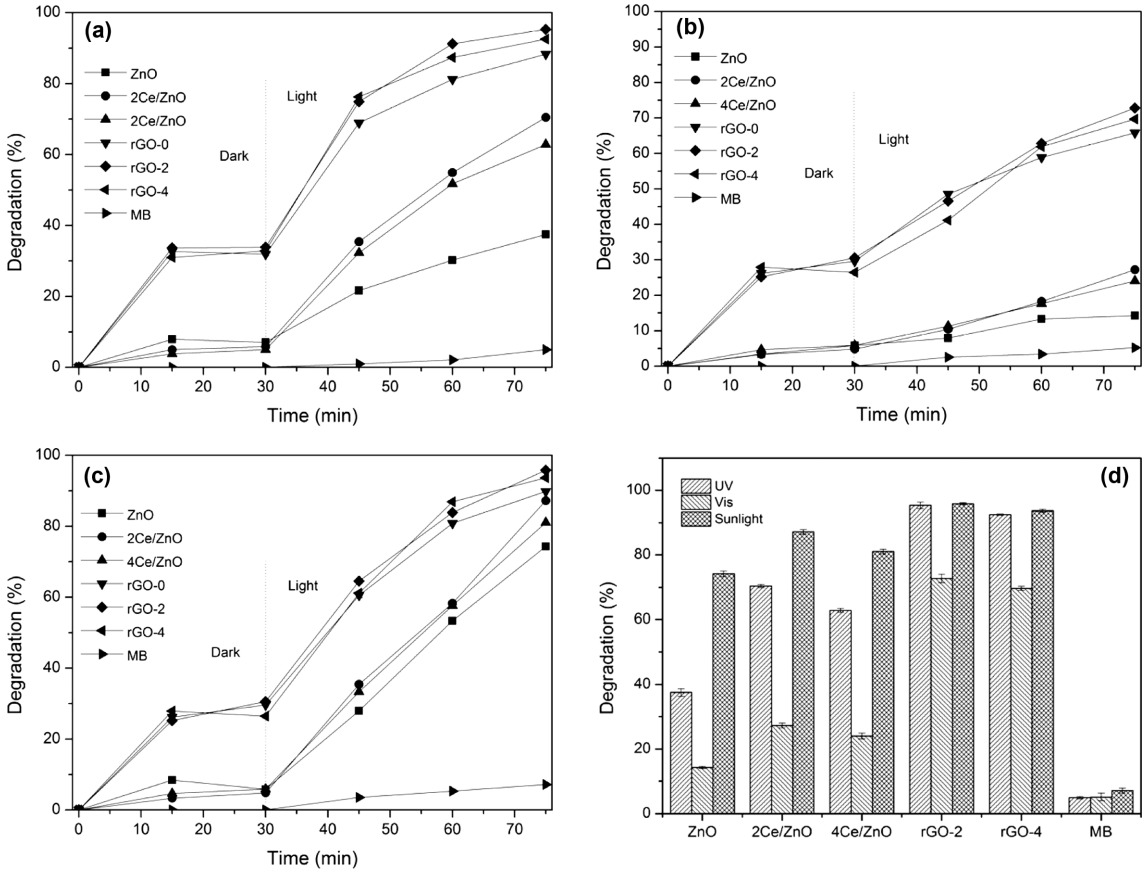

Fig. 7. (a-c) the photocatalytic degradation of MB (10 mg/L) by ZnO, 2Ce/ZnO, 4Ce/ZnO, rGO-ZnO, rGO-2 and rGO-4 under the irradiation of UV, visible and sunlight. (d) A comparison of the final degradation of MB (10 mg/L) between ZnO, 2Ce/ZnO, 4Ce/ZnO, rGO-ZnO, rGO-2 and rGO-4 under the irradiation of UV, visible and sunlight.

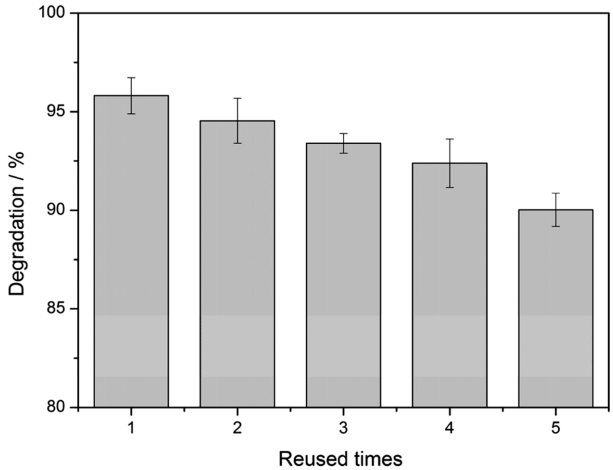

Fig. 8. Cycling runs in the degradation of MB in the presence of rGO-2 composite under sunlight irradiation.

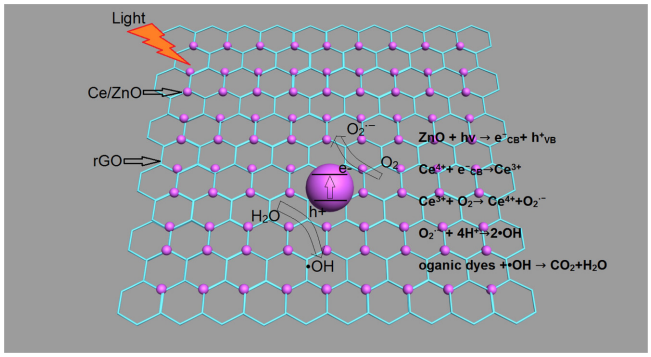

Fig. 9. Mechanism of the process of photodegradation.

can be transferred to rGO or trapped by Ce^{4+}, thus a lower recombination rate of photo-generated electron-hole pairs. After that, the electron is trapped by absorbed O_2 from the air to become the O^{2-}, and the water captures the hole to produce the •OH, which is the major series for the degradation of organic contamination. These free radicals can degrade the organic contamination as CO_2 and H_2O, due to its strong oxidability [46]. Once the adsorption-desorption equilibrium of MB on the photocatalyst surface is broken, the nearby MB is adsorbed immediately to reach a new equilibrium. Therefore, the synergistic effect between adsorption and photocatalysis endows the composites a higher photocatalytic activity, as shown in Fig. 8. In summary, improved visible light absorption, improvements in charge separation, efficient electron transfer, and large surface contact between reduced rGO-Ce/ZnO induced by enhanced adsorptivity of dyes are responsible for the highly efficient photocatalytic activity of the composites.

4. Conclusions

A quick and facile approach is proposed for preparation of rGO-Ce/ZnO composites. The prepared composites were investigated by XRD, SEM, FT-IR, PL, DRS techniques. It has been demonstrated that rGO-2 shows the significantly improved photocatalytic activity compared to the Ce/ZnO, pristine ZnO under UV, visible-light and sunlight irradiation. This highly enhanced photoactivity of the composite is likely to be ascribed to great adsorption of dyes, retarded charge recombination rate, fast transfer processes and enhanced visible light absorption. Hence, the rGO-Ce/ZnO composites pave the way for applications in water treatment fields.

References

1. Kim, K. H. and Ihm, S. K., "Heterogeneous Catalytic Wet Air Oxidation of Refractory Organic Pollutants in Industrial Wastewaters: A Review," *Hazard Mater*., **186**, 16-34(2011).
2. Shi, Z. L., Du, C. and Yao, S. H., "Preparation and Photocatalytic Activity of Cerium Doped Anatase Titanium Dioxide Coated Magnetite Composite," *J. Taiwan. Inst. Chem. E*., **42**, 652-657(2011).
3. Lia, X. Y., Wang, J., Yang, J. H., Lang, J. H., Lü, S. Q., Wei, M. B., Meng, X. W., Kou, C. L. and Li, X. F., "Comparison of Photocatalytic Activity of ZnO Rod Arrays with Various Diameter Sizes and Orientation," *J. Alloy. Compd*., **580**, 205-210(2013).
4. Liu, Y. M., Lv, H., Li, S. Q, Xing, X. Y. and Xi, G. X., "Preparation and Photocatalytic Property of Hexagonal Cylinder-like Bipods ZnO Microcrystal Photocatalyst," *Dyes and Pigments*., **95**, 443-449(2012).
5. Linsebigler, A. L., Lu, G. Q. and Yates, J. T., "Photocatalysis on TiO_2 Surfaces: Principles, Mechanisms, and Selected Results," *Chem. Rev*., **95**, 735-775(1995).
6. Rezaei, M., Habibi-Yangjeh, A., "Microwave-assisted Preparation of Ce-doped ZnO Nanostructures as An Efficient Photocatalyst," *Mater. Lett*., **110**, 53-56(2013).
7. Ahmada, M., Ahmed, E., Hong, Z. L., Khalid, N. R., Ahmed, W. and Elhissi, A., "Graphene-Ag/ZnO Nanocomposites as High Performance Photocatalysts Under Visible Light Irradiation," *J. Alloys. Compd.*, **577**, 717-727(2013).
8. Thiruvenkatachari, R., Vigneswaran, S. abd Moon, S., "A Review on UV/TiO_2 Photocatalytic Oxidation Process," *Korean J. Chem. Eng*., **25**(1), 64-72(2008).
9. Farzadkia, M., Rahmani, K., Gholami, M., Esrafili, A., Rahmani, A. and Rahmani, H., "Investigation of Photocatalytic Degradation of Clindamycin Antibiotic by Using Nano-ZnO Catalysts," *Korean J. Chem. Eng*., **31**(11), 2014-2019(2014).
10. Navarro, S., Fenoll, J., Vela. N., Ruiz, E. and Navarro, G., "Photocatalytic Degradation of Eight Sticides in Leaching Water by Use of ZnO Under Natural Sunlight," *J. Hazard. Mater*., **172**, 1303-1310(2009).
11. Yu, J. G, Xiang, Q. J. and Zhou, M. H., "Preparation, Characterization and Visible-light-driven Photocatalytic Activity of Fe-doped Titania Nanorods and First-principles Study for Electronic Structures," *Appl. Catal. B-Environ*., **90**, 595-602(2009).
12. Fu, H., Xu, T., Zhu, S. and Zhu, Y., "Photocorrosion Inhibition and Enhancement of Photocatalytic Activity for ZnO via Hybridization with C_{60}," *Environ. Sci. Technol*., **42**, 8064-8069(2008).
13. Chaudhari, S. P., Bodade, A. B., Chaudhari, and G. N., "Synthesis, Characterization and Photocatalytic Recital of Nest-like Zinc Oxide Photocatalyst," *Korean J. Chem. Eng*., **30**(11), 2001-2006(2013).
14. Li, Q., Li, H., Wang, R., Li, G., Yang, H. and Chen, R., *J. Alloys Comp*., **567**, 1(2013).
15. Zong, Y. Q., Li, Z., Wang, X. M., Ma, J. T. and Men, Y., "Synthesis and High Photocatalytic Activity of Eu-doped ZnO Nanoparticles," *Ceram. Int*., **40**, 10375-10382(2014).
16. Chang, C. J., Lin, C. Y. and Hsu, M. H., "Enhanced Photocatalytic Activity of Ce-doped ZnO Nanorods Under UV and Visible Light," *J. Taiwan. Inst. Chem. E.*, **45**, 1954-1963(2014).
17. Ba-Abbad, M. M., Kadhum, A. A. H., Mohamad, A. B., Takriff, M. S. and Sopian, K., "Visible Light Photocatalytic Activity of Fe^{3+}-doped ZnO Nanoparticle Prepared via Sol-gel Technique," *Chemosphere*., **91**, 1604-1611(2013).
18. Zhang, X. L., Zhao, J. L., Wang, S. G., Dai, H. T. and Sun, X. W., "Shape-dependent Localized Surface Plasmon Enhanced Photocatalytic Effect of ZnO Nanorods Decorated with Ag," *Int. J. Hydrogen. Energ*., **39**, 8238-8245(2014).
19. Peng, F., Zhu, H. C., Wang, H. J. and Yu, H., "Preparation of Ag-sensitized ZnO and Its Photocatalytic Performance Under Simulated Solar Light," *Korean J. Chem. Eng*., **24**(6), 1022-1026(2007).
20. George, A., Sharma, S. K., Chawla, S., Malik, M. M. and Qureshi, M. S., "Detailed of X-raydiffraction and Photoluminescence Studies of Ce Doped ZnO Nanocrystals," *J. Alloys. Compd.*, **509**, 5942-5946(2011).
21. Ge, C., Xie, C. and Cai, S., "Preparation and Gas-sensing Properties of Ce-doped ZnO Thin-film Sensors by Dip-coating," *Mater. Sci. Eng. B*., **137**, 53-58(2007).
22. Ma, T. Y., Yuan, Z. Y. and Cao, J. L., "Hydrangea-like Meso-/macroporous ZnO-CeO_2 Binary Oxide Materials: Synthesis, Photocatalysis and CO Oxidation," *Eur. J. Inorg. Chem*., **5**, 716-724(2010).
23. Faisal, M., Khan, S. B., Rahman, M. M., Jamal, A., Akhtar, K. and Abdullah, M. M., "Role of ZnO-CeO_2 Nanostructures as a Photocatalyst and Chemisensor," *J. Mater. Sci. Technol*., **29**, 594-600 (2011).
24. Du, F. L., Wang, N., Zhang, D. M. and Shen, Y. Z., "Preparation, Characterization and Infrared Emissivity Study of Ce-doped ZnO Films," *J. Rare Earths*., **28**, 391-395(2010).
25. Karunakaran, C., Gomathisankar, P. and Manikandan, G., "Preparation and Characterization of Antimicrobial Ce-doped ZnO Nanoparticles for Photocatalytic Detoxification of Cyanide," *Mater. Chem. Phys*., **123**, 585-594(2010).
26. Ying, L. A., Liu, J., Mo, L., Lou, H. and Zheng, X., "Hydrogen Production by Oxidative Steam Reforming of Methanol Over Ce_{1-x} Zn_xO_y Catalysts Prepared by Combustion Method," *Int. J. Hydrogen Energy*., **37**, 1002-1006(2012).
27. Yu, X. Q., Huo, Y. J., Yang, J., Chang, S. J., Ma, Y. S. and Huang, W. X., "Reduced Graphene Oxide Supported Au Nanoparticles as an Efficient Catalyst for Aerobic Oxidation of Benzyl Alcohol," *Appl. Surf. Sci*., **280**, 450-455(2013).
28. Nguyen-Phan, T. D., Pham, V. H., Yun, H., Kim, E. J., Hur, S. H., Chung, J. S. and Shin, E. W., "Influence of Heat Treatment on Thermally-reduced Graphene Oxide/TiO_2 Composites for Photocatalytic Applications," *Korean J. Chem. Eng*., **28**(12), 2236-2241(2011).

29. Li, X. Q., Zhang, T. Y., Gu, S. W., Kang, S. Z., Li, G. D. and Mu, J., "Reduced GO/potassium Niobate Composite Nanoscrolls with Enhanced Photocatalytic Activity for Dye Degradation," *Sep. Purif. Technol*., **108**, 139-142(2013).
30. Xu, S. H., Fu, L., Song, T., Pham, H., Yu, A., Han, F. G. and Chen, L., "Preparation of ZnO Flower/reduced Graphene Oxide Composite with Enhanced Photocatalytic Performance Under Sunlight," *Ceram. Int*., **41**, 4007-4013(2015).
31. Li, B. X., Liu, T. X., Wang, Y. F. and Wang, Z. F., "ZnO/graphene-oxide Nanocomposite with Remarkably Enhanced Visible-light-driven Photocatalytic Performance," *J. Colloid. Interf. Sci*., **377**, 114-121(2012).
32. Liu, S. Z., Sun, H. Q., Suvorova, A. and Wang S. B., "One-pot Hydrothermal Synthesis of ZnO-reduced GO Composites Using Zn Powders for Enhanced Photocatalysis," *Chem. Eng. J.*, **229**, 533-539(2013).
33. Lv, T., Pan, L.K., Liu, X. J., Lu, T., Zhu, G. and Sun, Z., "Enhanced Photocatalytic Degradation of Methylene Blue by ZnO-reduced Graphene Oxide Composite Synthesized via Microwave-assisted Reaction," *J. Alloy. Compd.*, **509**, 10086-10091(2011).
34. Ameen, S., Akhtar, M. S., Seo, H. K. and Shin, H. S., "Advanced ZnO-GO Nanohybrid and Its Photocatalytic Applications," *Mater. Lett*., **100**, 261-265(2013).
35. Zhou, X., Shi, T. J. and Zhou, H. O., "Hydrothermal Preparation of ZnO-reduced Graphene Oxide Hybrid with High Performance in Photocatalytic Degradation," *Appl. Surf. Sci*., **258**, 6204-6211(2012).
36. Neppolian, B., Bruno, A. and Bianchi, C. L., "Muthupandian Ashokkumar. Graphene Oxide Based Pt-TiO_2 Photocatalyst: Ultrasound Assisted Synthesis, Characterization and Catalytic Efficiency, Characterization and Catalytic Efficiency," *Ultrason. Sonochem.*, **19**, 9-15(2012).
37. Willam, S. Hummers, J. R. and Richarde, E., "Offema. Preparation of Graphitic Oxide," *J. Am. Chem. Soc*., 1339-1339(1958).
38. Park, S., Lee, K. S., Bozoklu, G., Cai, W. W., Nguyen, S. T. and Ruoff, R. S., "Graphene Oxide Papers Modified by Divalent Ions-Enhancing Mechanical Properties via Chemical Cross-Linking," *ACS Nano*., **2**, 572-578(2008).
39. Li, J., Zhou, S. L., Hong, G. B. and Chang, C. T., "Hydrothermal Preparation of P25-graphene Composite with Enhanced Adsorption and Photocatalytic Degradation of Dyes," *ChE. Eng. J*., **219**, 486-491(2013).
40. Karunakaran, C., Gomathisankar, P. and Manikandan, G., "Preparation and Characterization of Antimicrobial Ce-doped ZnO Nanoparticles for Photocatalytic Detoxification of Cyanide," *Mater. Chem. Phys*., **123**, 585-594(2010).
41. Ahmad, M., Ahmed, E., Hong, Z. L., Khalid, N. R., Ahmed, W. and Elhissi, A., "Graphene-Ag/ZnO Nanocomposites as High Performance Photocatalysts Under Visible Light Irradiation," *J. Alloys. Compd.*, **577**, 717-727(2013).
42. Zhang, H., Lv, X. J., Li, Y. M., Wang, Y. and Li, J. H., P25-Graphene Composite as a High Performance Photocatalyst," *ACS Nano.*, **4**, 380-386(2010).
43. Bai, S. and Shen, X. P., "Graphene-inorganic Nanocomposites," *RSC Advances.*, **2**, 64-98(2012).
44. Liu, S., Tian, J. Q., Wang, L. and Sun, X. P., "A Method for the Production of Reduced Graphene Oxide Using Benzylamine as a Reducing and Stabilizing Agent and Its Subsequent Decoration with Ag Nanoparticles for Enzymeless Hydrogen Peroxide Detection," *Carbon*., **49**, 3158-3164(2011).
45. Ghasemia, S., Setayesh, S. R., Habibi-Yangjehb, A., Hormozi-Nezhad, M. R. and Gholami, M. R., "Assembly of CeO_2-TiO_2 Nanoparticles Prepared in Room Temperature Ionic Liquid on Graphene Nanosheets for Photocatalytic Degradation of Pollutants," *J. Hazard. Mater*., **199-200**, 170-178(2012).
46. Zhou, X., Shi, T. J. and Zhou, H. O., "Hydrothermal Preparation of ZnO-reduced Graphene Oxide Hybrid with High Performance in Photocatalytic Degradation," *Appl. Surf. Sci*., **258**, 6204-6211(2012).